Calculating ground state energy of many-body systems using Variational Quantum Eigensolver

Carl Fredrik Nordbø Knutsen[1] and August Gude[2]

[1] Department of Mathematics, University of Oslo, [2] Department of Physics, University of Oslo

(Dated: June 3, 2023)

In this work, we use the VQE algorithm to calculate the ground state energy of many-body Hamiltonians. We start with simple Hamiltonians of two and four dimensions which we rewrite as quantum circuits of one and two qubits, respectively. The ground state energy is calculated both with simulations of quantum devices and, for the one qubit case, with IBM's quantum devices. We study the dependence on the interaction strength in the many-body Hamiltonian for both systems and see a clear level-crossing in the ground state energy. We also make calculations on the Lipkin model of total spin $J = 1$ and $J = 2$. We map the Lipkin model over to quantum circuits via both an individual spin scheme and a coupled spin scheme. The coupled spin mapping requires half as many qubits as the individual spin mapping. For the system of total spin $J = 2$, we find the exact ground state energy only for the coupled spin mapping. The failure of the individual spin mapping can be attributed to our ansatz selection failing to represent the ground state's intrinsic symmetries. The code used to generate the results and our data can be found at https://github.com/augude/FYS4411—Project-2.

I. INTRODUCTION

In a lecture in 1982, Richard P. Feynman talked about the usage of computers to simulate physics. In particular, he talked about simulations of quantum mechanics:

> (...) how can we simulate the quantum mechanics? There are two ways that we can go about it. We can give up on our rule about what the computer was, we can say: Let the computer itself be built of quantum mechanical elements which obey quantum mechanical laws. Or we can turn the other way and say: Let the computer still be the same kind that we thought of before - a logical, universal automaton; can we imitate this situation? [4]

He answered the latter question with "no": The hidden-variable problem does not allow for a classical representation of quantum mechanics. The way to simulate quantum mechanics is therefore by using computers "built of quantum mechanical elements which obey quantum mechanical laws", commonly referred to as quantum computers. Today, 40 years after Feynman's lecture, huge processes are made in the field of quantum computing, however, the devices are still not capable of accurately simulating large quantum systems. The quantum computers of today have a limited number of qubits and too few physical qubits to implement robust error correction schemes, and are therefore not yet suited for applications such as prime or unordered search [12]. However, algorithms that work with Noisy Intermediate Scale Quantum (NISQ) devices are actively studied. Among the promising examples of algorithms that work with NISQ devices is the Variational Quantum Eigensolver (VQE) [9].

In this work, we aim to use the VQE algorithm for estimating the ground state energy of many-body systems. We start with simple Hamiltonians with a tuneable many-body interaction, before turning to the Lipkin model. The Lipkin model was introduced in 1964 as a model for many-body problems in quantum mechanics and is simple enough to have exact solutions, while still incorporating a nontrivial interaction [8]. We will closely follow the work of Hlatshwayo et.al [5].

In section II, we introduce various toy models for many-body problems, including the Lipkin model. We also outline the VQE algorithm. Further, the mapping of the many-body Hamiltonians to quantum circuits and implementation of the VQE algorithm are found in section III. We present the results of our computations in section IV.

II. BACKGROUND

1. Simple many-body Hamiltonians

In general, many-body Hamiltonians can be split into a non-interacting and an interacting term:

$$H = H_0 + H_I,$$

where H_0 is the non-interacting solution and H_I incorporates the two-body part of the system. In our study, we will first focus on a two-dimensional system where the non-interacting part H_0 can be represented as a diagonal matrix characterized by the non-interacting energies

$$H_0 |0\rangle = E_0 |0\rangle$$
$$H_0 |1\rangle = E_1 |1\rangle .$$

Here, we are working with the standard basis of $\mathbb{C}^2$. Similarly, the interaction term can be represented as a 2×2 Hermitian matrix, with elements

$$H_I = \begin{pmatrix} V_{11} & V_{12} \\ V_{21} & V_{22} \end{pmatrix}.$$

The matrices can be rewritten in terms of the Pauli matrices as

$$H_0 = \mathcal{E} I + \Omega Z,$$

and

$$H_I = cI + \omega_z Z + \omega_z Z,$$

where $\mathcal{E} = (E_1 + E_2)/2$, $\Omega = (E_1 - E_2)/2$, $c = (V_{11} + V_{22})/2$, $\omega_z = (V_{11} - V_{22})/2$, and $\omega_x = V_{21}^* = V_{12}$. To study the effect of the interaction, we introduce a strength parameter λ and let the interaction depend linearly on λ, which takes values in $[0, 1]$. Thus, the full two-dimensional Hamiltonian can be rewritten as

$$H = (\mathcal{E} + \lambda c)\, I + (\Omega + \lambda \omega_z)\, Z + \lambda \omega_x X. \tag{1}$$

We will also extend our study of simple many-body Hamiltonians to a four-dimensional case. Here, the non-interacting part is again given by its energy eigenvalues

$$H_0 |00\rangle = \epsilon_{00} |00\rangle,$$
$$H_0 |01\rangle = \epsilon_{01} |01\rangle,$$
$$H_0 |10\rangle = \epsilon_{10} |10\rangle,$$
$$H_0 |11\rangle = \epsilon_{01} |11\rangle,$$

where we have chosen our computational basis to be the standard basis in $\mathbb{C}^2 \otimes \mathbb{C}^2$. In the four-dimensional case, our model for the interacting term in the Hamiltonian is given by

$$H_I = H_z Z \otimes Z + H_x X \otimes X,$$

which we abbreviate to

$$H_I = H_z ZZ + H_x XX,$$

where tensor products between one-body operators are implied. The non-interacting part of the Hamiltonian can be rewritten in terms of Pauli matrices as

$$H_0 = \alpha II + \beta IZ + \gamma ZI + \delta ZZ,$$

where the coefficients are given by

$$\alpha = (\epsilon_{00} + \epsilon_{01} + \epsilon_{10} + \epsilon_{11})/4,$$
$$\beta = (\epsilon_{00} - \epsilon_{01} + \epsilon_{10} - \epsilon_{11})/4,$$
$$\gamma = (\epsilon_{00} + \epsilon_{01} - \epsilon_{10} - \epsilon_{11})/4,$$
$$\delta = (\epsilon_{00} - \epsilon_{01} - \epsilon_{10} + \epsilon_{11})/4.$$

As above, we introduce a strength parameter λ to control the interactive part of the Hamiltonian. Combining the expressions for the non-interactive and the interaction terms in the Hamiltonian gives

$$H = \alpha II + \beta IZ + \gamma ZI + (\delta + \lambda H_z)\, ZZ + \lambda H_x XX. \tag{2}$$

2. The Lipkin model

The Lipkin model is a simple yet powerful model used in many-body physics to study the collective behavior of interactive particles [8].

1. Physical assumptions

In the Lipkin model, we consider N spin-1/2 fermions that distribute over two energy levels, $E = \pm\epsilon/2$, which are both N-fold degenerate. The particles interact through a pairwise interaction, which in general can be either attractive or repulsive, however, we will only consider an attractive potential in our study. Moreover, it is assumed that the total spin of the system is conserved, even when the particles change their individual spin quantum numbers. The spin of the particles determines whether the particle is in the upper or lower energy level.

In each energy level, there are N positions for particles, enumerated by $p = 1, \ldots, N$. One assumes that only one particle can occupy a single position p, i.e., there can either be a particle at position p with spin up or a particle at position p with spin down, but not both. Thus, every slot is uniquely defined by two quantum numbers, the particle position p and the spin σ. A sketch of a possible particle distribution for a system of total spin $J = 2$ is shown in Fig. (1). In the figure, the fermions at position $p = 1$ and $p = 4$ have spin up and are in the upper energy level, while the fermions at positions $p = 2$ and $p = 3$ have spin down and are in the lower energy level. In the second quantization

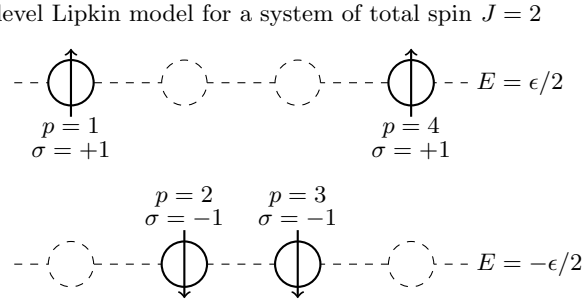

FIG. 1. A sketch of the half-filled Lipkin model for total spin $J = 2$ in a configuration where two fermions have energy $E = \epsilon/2$ and two fermions have energy $E = -\epsilon/2$. Occupied slots are marked with filled circles, while empty slots are marked with dashed circles. The spins of the fermions are marked with arrows, and the quantum numbers for each particle (position p and spin σ) are printed together with each occupied slot.

formalism, the Lipkin Hamiltonian is given by

$$H = \frac{\epsilon}{2}\sum_{\sigma,p}\sigma a^\dagger_{p,\sigma}a_{p,\sigma} - \frac{V}{2}\sum_{\sigma,p,p'} a^\dagger_{p,\sigma}a^\dagger_{p',\sigma}a_{p',-\sigma}a_{p,-\sigma} - \frac{W}{2}\sum_{\sigma,p,p'} a^\dagger_{p,\sigma}a^\dagger_{p',-\sigma}a_{p',\sigma}a_{p,-\sigma}, \tag{3}$$

where ϵ determines the single particle energy and V and W control the strength of the interactions. In the second quantization formalism, $a^\dagger_{\sigma,p}$ and $a_{\sigma,p}$ are creation and annihilation operators for slot (p,σ), respectively. The first term in the Lipkin Hamiltonian is a non-interactive diagonal operator. The interaction term associated with V, called the V-scattering term, is responsible for scattering two particles from the upper energy level to the lower energy level, or vice versa. The interaction term associated with W, called the W-scattering term, is responsible for interchanging the spins of two particles, ie. simultaneously scattering one particle up and another particle down, or vice versa. In terms of quasispin operators, Eq. (3) can be rewritten as

$$H = \frac{\epsilon}{2}J_z - \frac{V}{2}\left(J_+^2 + J_-^2\right) - \frac{W}{2}\left(J_+J_- + J_-J_+ - N\right), \tag{4}$$

where J_z is the operator associated with the spin in z-direction, $J_\pm$ are raising and lowering operators of the spin projection in z-direction and N is the number operator. One readily checks that the Hamiltonian commutes with the square of the total spin operator J^2, such that the total spin of the system is conserved, as desired.

For the simplest case of total spin $J = 1$, there are three possible states which in terms of the total spin and the spin component in the z-direction, $|J, J_z\rangle$, can be labeled

$$|1,-1\rangle, |1,0\rangle, \text{ and } |1,1\rangle.$$

The first state corresponds to both particles having spin down, the second state corresponds to one particle with spin up and one with spin down, and the last state corresponds to both particles having spin up. Using the Condon-Shortley phase convention [2], the act of a raising or lowering operator on one of the states is

$$J_\pm |J, J_z\rangle = \sqrt{J(J+1) - J_z(J_z \pm 1)}\,|J, J_z \pm 1\rangle. \tag{5}$$

Hence, the action of the Hamiltonian on the possible states in the case where $W = 0$ is

$$\begin{aligned} H_{J=1}|1,-1\rangle &= -\epsilon|1,-1\rangle - V|1,1\rangle, \\ H_{J=1}|1,0\rangle &= 0, \\ H_{J=1}|1,1\rangle &= \epsilon|1,1\rangle - V|1,-1\rangle. \end{aligned} \tag{6}$$

By identifying the states $|J, J_z\rangle$ with the standard basis vectors in $\mathbb{C}^3$, the Hamiltonian can be represented as

$$H_{J=1} = \begin{pmatrix} -\epsilon & 0 & -V \\ 0 & 0 & 0 \\ -V & 0 & \epsilon \end{pmatrix}.$$

Similarly, for the case of total spin $J = 2$, the possible states are

$$|2,-2\rangle, |2,-1\rangle, |2,0\rangle, |2,1\rangle, \text{ and } |2,2\rangle,$$

and the action of the Hamiltonian on these states in the case where $W = 0$ is

$$\begin{aligned} H_{J=2}|2,-2\rangle &= -2\epsilon|2,-2\rangle + \sqrt{6}V|2,0\rangle, \\ H_{J=2}|2,-1\rangle &= -\epsilon|2,-1\rangle + 3V|2,1\rangle, \\ H_{J=2}|2,0\rangle &= \sqrt{6}V|2,-2\rangle + \sqrt{6}V|2,2\rangle, \\ H_{J=2}|2,1\rangle &= \epsilon|2,1\rangle + 3V|2,-1\rangle, \\ H_{J=2}|2,2\rangle &= 2\epsilon|2,2\rangle + \sqrt{6}V|2,0\rangle. \end{aligned} \tag{7}$$

In matrix form, the Hamiltonian can be represented as

$$H_{J=2} = \begin{pmatrix} -2\epsilon & 0 & \sqrt{6}V & 0 & 0 \\ 0 & -\epsilon & 0 & 3V & 0 \\ \sqrt{6}V & 0 & 0 & 0 & \sqrt{6}V \\ 0 & 3V & 0 & \epsilon & 0 \\ 0 & 0 & \sqrt{6}V & 0 & 2\epsilon \end{pmatrix}.$$

2. *Individual spin mapping*

When simulating the Lipkin Hamiltonian on a quantum computer, the basis states must be rewritten in terms of qubit basis states, and the Hamiltonian must be rewritten in terms of quantum gates. For both the system of total spin $J = 1$ and $J = 2$, the spin basis states can be mapped to a computational qubit basis by

$$|\downarrow\downarrow\rangle, |\downarrow\uparrow\rangle, |\uparrow\downarrow\rangle, |\uparrow\uparrow\rangle \mapsto |00\rangle, |01\rangle, |10\rangle, |11\rangle$$

for the case of $J = 1$, and similarly for $J = 2$ with computational basis states in $C^{2^{\otimes 4}}$. This is the individual spin basis mapping, as each fermion is represented by a qubit. When rewriting the Hamiltonian to quantum gates, we use that the quasispin operators are connected to the Pauli matrices by

$$J_z = \frac{1}{2}\sum_{n=0}^{N-1} Z_n, \tag{8}$$

$$J_\pm = \sum_{n=0}^{N-1} \frac{X_n \pm iY_n}{\sqrt{2}}, \tag{9}$$

where N is the number of qubits and P_n is understood to be a Pauli gate acting solely on qubit n. Using Eq.

(8) and Eq. (9), the Lipkin Hamiltonian given in terms of quasispin operators can be rewritten in terms of Pauli operators as

$$H = \frac{\epsilon}{2}\sum_n Z_n - \frac{V}{2}\sum_{n<m}(X_nX_m - Y_nY_m) - \frac{W}{2}\sum_{n<m}(X_nX_m + Y_nY_m)\,. \tag{10}$$

In particular, the Hamiltonians for the cases of $J = 1$ ($N = 2$ qubits) and $J = 2$ ($N = 4$ qubits) with no W-scattering are given by

$$H_{J=1} = \frac{\epsilon}{2}(ZI + IZ) - \frac{V}{2}(XX - YY)\,, \tag{11}$$

and

$$\begin{aligned} H_{J=2} = {} & \frac{\epsilon}{2}(ZIII + IZII + IIZI + IIIZ) \\ & - \frac{V}{2}(XXII + XIXI + XIIX \\ & \quad + IXXI + IXIX + IIXX) \\ & + \frac{V}{2}(YYII + YIYI + YIIY \\ & \quad + IYYI + IYIY + IIYY), \end{aligned} \tag{12}$$

respectively. As above, tensor products are implied between Pauli matrices.

3. *Coupled spin mapping*

The individual spin basis mapping of the Lipkin model uses $N = 2J$ qubits to represent a system of total spin J. However, when neglecting the W-scattering term in the Hamiltonian, more efficient mapping schemes exist. Since the V-scattering term in the Hamiltonian raises or lowers the spin of *two* fermions simultaneously, the only allowed values for the spin in the z-direction are $J_z = -J, -J+2, \ldots, J-2, J$. For the system of total spin $J = 1$, the only possible states are therefore $|1,-1\rangle$ and $|1,1\rangle$. These states can be represented by a single qubit by setting

$$|1,-1\rangle\,, |1,1\rangle \mapsto |0\rangle\,, |1\rangle\,.$$

This coupled spin mapping requires half of the qubits needed for the individual spin mapping. In this encoding scheme, the act of the Hamiltonian on the coupled spin states given by Eq. (6) can be rewritten as

$$\begin{aligned} H_{J=1}\,|0\rangle &= -\epsilon\,|0\rangle - V\,|1\rangle \\ H_{J=1}\,|1\rangle &= \epsilon\,|1\rangle - V\,|0\rangle\,, \end{aligned}$$

which implies that the Hamiltonian for total spin $J = 1$ in the coupled spin mapping is given by

$$H_{J=1} = -\epsilon Z - VX. \tag{13}$$

Similarly, for a system of total spin $J = 2$, the possible states are $|2,-2\rangle\,, |2,0\rangle$, and $|2,2\rangle$, which can be represented by a system of two qubits by mapping

$$|2,-2\rangle\,, |2,0\rangle\,, |2,2\rangle \mapsto |00\rangle\,, |10\rangle\,, |11\rangle\,.$$

The state $|01\rangle$ is missing from our encoding scheme since we are only interested in spin states where J_z is an even number. With these basis states, the action of the Hamiltonian on the coupled spin states given by Eq. (7) can be rewritten as

$$\begin{aligned} H_{J=2}\,|00\rangle &= -2\epsilon\,|00\rangle + \sqrt{6}V\,|10\rangle\,, \\ H_{J=2}\,|10\rangle &= \sqrt{6}V\,|00\rangle + \sqrt{6}V\,|11\rangle\,, \\ H_{J=2}\,|11\rangle &= 2\epsilon\,|11\rangle + \sqrt{6}V\,|10\rangle\,, \end{aligned}$$

which, following the work of [5], can be rewritten in terms of Pauli gates as

$$H_{J=2} = -\epsilon\,(ZI + IZ) - \frac{\sqrt{6}}{2}V\,(XI + IX + XZ - ZX)\,. \tag{14}$$

3. The VQE algorithm

The VQE algorithm is based on the variational principle, which states that the lowest energy eigenvalue E_0 of a Hamiltonian H satisfies

$$E_0 \leq \langle\psi(\boldsymbol{\theta})|\,H\,|\psi(\boldsymbol{\theta})\rangle\,, \tag{15}$$

for all parameterized quantum states $|\psi(\boldsymbol{\theta})\rangle$. If every state is accessible, the ground state energy is given exactly by

$$E_0 = \min_{\boldsymbol{\theta}} \langle\psi(\boldsymbol{\theta})|\,H\,|\psi(\boldsymbol{\theta})\rangle\,.$$

The VQE algorithm consists of several steps, partially done on a classical computer:

1. A parameterized ansatz for the quantum state is implemented on a quantum computer.
2. The ansatz is measured in a given measurement basis.
3. Postprocessing on a classical computer converts the measurement outcomes to an expectation value.
4. Classical minimization algorithms are used to update the variational parameters.

The updated variational parameters are then sent back to the quantum computer, and the process is repeated until the optimal variational parameters are found. Each step in the VQE algorithm can be implemented in various ways, which is discussed in great detail in [12]. The next section covers our implementation of the VQE algorithm, tailored to many-body Hamiltonians.

III. IMPLEMENTATION

1. Ansatz selection and state preparation

The first, and arguably most crucial part of the VQE algorithm is the selection of a suitable ansatz for the quantum state. When choosing the ansatz, both the expressibility and the trainability of the ansatz need to be considered. That is, for the lowest energy eigenvalue to be found, the span of the ansatz must contain the state that globally minimizes the expectation value of the Hamiltonian. However, one also needs to consider the computational cost of performing an optimization with many variational parameters. Thus, a well-suited ansatz needs to be easy to train, while simultaneously spanning a sufficiently large subset of the Hilbert space if the lowest eigenvalue is to be found in a reasonable time.

In this study, we opt for a hardware-efficient ansatz that is easily prepared on a quantum device. The hardware-efficient ansatz is prepared by repeated blocks of single qubit rotation gates and ladders of entanglement gates [12]. In particular, we act on each qubit separately by two rotation gates along the X-axis and Y-axis before entangling the qubits together with controlled-NOT gates. The rotation gates ensure that every single-qubit state on the Bloch sphere is accessible, and the controlled-NOT gates ensure that entangled many-body states are also accessible. The hardware-efficient ansatz requires at least $2N$ variational parameters. The circuit needed for the preparation of an ansatz for $N = 2$ qubits is given in Fig. (2). In the figure, both qubits

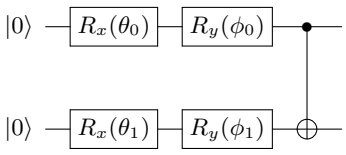

FIG. 2. Circuit used to prepare the hardware-efficient ansatz for a system of $N = 2$ qubits.

are initialized in the state $|0\rangle$. Then, parameterized rotational gates are applied, where the gates are given by

$$R_x(\theta_n) = e^{i\theta_n/2X} = \cos(\theta_n/2)\, I - i \sin(\theta_n/2)\, X,$$

$$R_y(\phi_n) = e^{i\phi_n/2Y} = \cos(\phi_n/2)\, I - i \sin(\phi_n/2)\, Y.$$

Lastly, to incorporate entanglement, an X-gate controlled by the first qubit is applied to the second qubit.

For the coupled spin mapping of the Lipkin model, we have utilized the symmetries of the system to reduce the dimension of the problem. For the VQE algorithm to find the global minimum, the ansatz must have the same symmetries as the ground state. We know that the ground state of the Lipkin model for $J = 2$ is a combination of the states $|00\rangle, |10\rangle$, and $|11\rangle$, but *not* $|01\rangle$. The ansatz must be a combination of the same states, and we construct this by the circuit given in Fig. (3). Upon analyzing the circuit in the figure, we see that

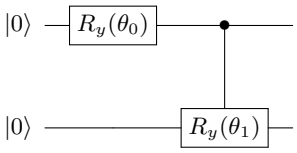

FIG. 3. Circuit used to prepare the ansatz for the Lipkin model for total spin $J = 2$ when using the coupled spin basis

the ansatz is given by

$$|\psi(\theta_0, \theta_1)\rangle = \cos(\theta_0/2)\,|00\rangle + \sin(\theta_0/2)\cos(\theta_1/2)\,|10\rangle + \sin(\theta_0/2)\sin(\theta_1/2)\,|11\rangle,$$

which indeed has the same symmetries as the ground state.

2. Measurement of the Hamiltonian

The VQE algorithm aims to find the lowest eigenvalue of the Hamiltonian by minimizing $\langle\psi(\boldsymbol{\theta})|\, H\, |\psi(\boldsymbol{\theta})\rangle$. However, a quantum circuit does not return the expectation value of the Hamiltonian directly, but rather a measurement outcome. The conversion between measurement outcomes and expectation values depends on the choice of the basis of measurement. When working with the standard computational basis, it is common to use $\mathcal{M} = Z$ as the measurement basis for the single-qubit case, and $\mathcal{M} = Z \otimes I^{\otimes N-1}$ as the measurement basis for the general case of N qubits. The many-body Hamiltonians in this study, Eq. (1), Eq. (2), Eq. (11), and Eq. (12), contain strings of Pauli gates of length corresponding to the number of qubits in the system. The Pauli strings need to be rewritten in terms of the measurement basis before measuring to calculate the expectation values. We denote Pauli strings of length N by $\mathcal{P} = \bigotimes_{n=0}^{N-1} P_i$, where P_i is either a X, Y, Z or I acting on qubit n. By the spectral theorem, any Pauli string can be rewritten in terms of the measurement basis $\mathcal{M}$ as

$$\mathcal{P} = U_{\mathcal{P}}^{\dagger} \mathcal{M} U_{\mathcal{P}}, \tag{16}$$

for some unitary operators $U_{\mathcal{P}}$ [3]. Thus, to measure a Pauli string $\mathcal{P}$ in the basis $\mathcal{M}$, one first has to apply the unitary operator $U_{\mathcal{P}}$ to rotate to the measurement basis. Operators for Pauli strings of length 1 and 2 are provided by Hundt [6], of which the ones relevant for our many-body models are listed in table Tab. (I). In the table, H is the Hadamard matrix, SWAP interchanges the probability amplitude for two qubits, $CX_{1,0}$ is a X-gate applied to the first qubit, controlled by the second, and S is the

TABLE I. Operators for measuring Pauli strings of length 1 in the basis Z, and Pauli strings of length 2 in the basis $Z \otimes I$.

Pauli string $\mathcal{P} = \bigotimes_{n=0}^{N-1} P_i$	Operator $U_\mathcal{P}$
X	H
$Z \otimes I$	$I \otimes I$
$I \otimes Z$	SWAP
$X \otimes I$	$H \otimes I$
$I \otimes X$	$(H \otimes I)\,\mathrm{SWAP}$
$Y \otimes I$	$HS^\dagger \otimes I$
$I \otimes Y$	$\left(HS^\dagger \otimes I\right)\mathrm{SWAP}$
$Z \otimes Z$	$CX_{1,0}$
$X \otimes X$	$CX_{1,0}\,(H \otimes H)$
$Y \otimes Y$	$CX_{1,0}\left(HS^\dagger \otimes HS^\dagger\right)$
$Z \otimes X$	$CX_{1,0}\,(I \otimes H)$
$X \otimes Z$	$CX_{1,0}\,(I \otimes H)\,\mathrm{SWAP}$

phase gate. The operators from Hundt are sufficient for our first two simple models of many-body interactions and the Lipkin model of total spin $J = 1$, however, the Lipkin model of total spin $J = 2$ with the individual spin mapping involves Pauli strings of length 4. In total, the Lipkin Hamiltonian $H_{J=2}$ without W-scattering contains 16 Pauli strings of length 4, which need to be rotated to the measurement basis $\mathcal{M} = Z \otimes I \otimes I \otimes I$. Since the Lipkin model acts at maximally two qubits at a time, the necessary four-qubit operators can be constructed by combining two two-qubit operators. We list the four-qubit operators needed for the Lipkin model with spin $J = 2$ in Tab. (II). The quantum circuit used for measuring the Pauli string $\mathcal{P}$ is shown in Fig. (4). For the first many-body models with Pauli strings of lengths one and two, we need to construct two and five circuits to calculate the expectation values, respectively. With the individual spin basis mapping, the Lipkin model of total spin $J = 1$ requires four quantum circuits, and the Lipkin model of total spin $J = 2$ requires 16 circuits.

TABLE II. Operators for measuring Pauli strings of length 4 in the basis $Z \otimes I \otimes I \otimes I$.

Pauli string $\mathcal{P} = \bigotimes_{n=0}^{N-1} P_i$	Operator $U_\mathcal{P}$
$Z \otimes I \otimes I \otimes I$	$I \otimes I \otimes I \otimes I$
$I \otimes Z \otimes I \otimes I$	$U_{IZ} \otimes I \otimes I$
$I \otimes I \otimes Z \otimes I$	$U_{IZII}\,(I \otimes U_{IZ} \otimes I)$
$I \otimes I \otimes I \otimes Z$	$U_{IIZI}\,(I \otimes I \otimes U_{IZ})$
$Z \otimes I \otimes Z \otimes I$	$(CX_{1,0} \otimes I \otimes I)\,(\mathrm{SWAP} \otimes I \otimes I)$
$X \otimes X \otimes I \otimes I$	$U_{XX} \otimes I \otimes I$
$X \otimes I \otimes X \otimes I$	$U_{ZIZI}\,(U_{XI} \otimes U_{XI})$
$X \otimes I \otimes I \otimes X$	$U_{ZIZI}\,(U_{XI} \otimes U_{IX})$
$I \otimes X \otimes X \otimes I$	$U_{ZIZI}\,(U_{IX} \otimes U_{XI})$
$I \otimes X \otimes I \otimes X$	$U_{ZIZI}\,(U_{IX} \otimes U_{IX})$
$I \otimes I \otimes X \otimes X$	$U_{IIZI}\,(I \otimes I \otimes U_{XX})$
$Y \otimes Y \otimes I \otimes I$	$U_{YY} \otimes I \otimes I$
$Y \otimes I \otimes Y \otimes I$	$U_{ZIZI}\,(U_{YI} \otimes U_{YI})$
$Y \otimes I \otimes I \otimes Y$	$U_{ZIZI}\,(U_{YI} \otimes U_{IY})$
$I \otimes Y \otimes Y \otimes I$	$U_{ZIZI}\,(U_{IY} \otimes U_{YI})$
$I \otimes Y \otimes I \otimes Y$	$U_{ZIZI}\,(U_{IY} \otimes U_{IY})$
$I \otimes I \otimes Y \otimes Y$	$U_{IIZI}\,(I \otimes I \otimes U_{YY})$

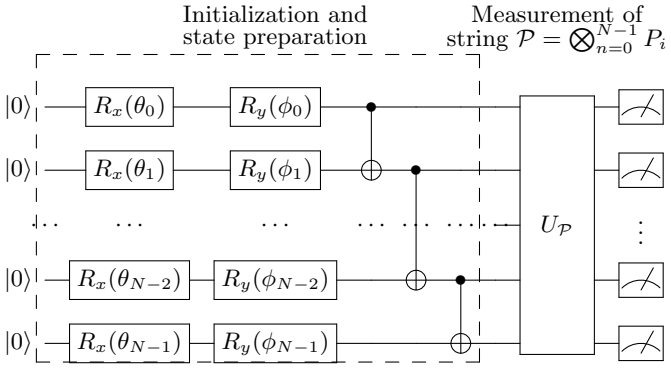

FIG. 4. Quantum circuit used for initializing a hardware-efficient ansatz and measuring the Pauli string $\mathcal{P}$ in the basis $\mathcal{M}$.

3. Calculation of expectation values

After constructing the ansatz and measuring the Pauli strings on a quantum computer, the measurement outcomes are sent to a classical computer for post-processing to calculate the expectation values. In the measurement basis $\mathcal{M} = Z \otimes I^{\otimes(N-1)}$, the possible eigenvalues are $\lambda = +1$ and $\lambda = -1$. Analytically, the expectation value of Z for a state $|\phi\rangle = \alpha\,|0\rangle + \beta\,|1\rangle$ is

$$\langle Z \rangle = |\alpha|^2 - |\beta|^2.$$

In practice, the values of α and β are unknown quantities. However, by keeping count of the outcomes when measuring the state $|\phi\rangle$, the probabilities $|\alpha|^2$ and $|\beta|^2$ can be approximated by the relative frequency by which the states $|0\rangle$ and $|1\rangle$ are measured. Thus, we perform many measurements while keeping count of the outcomes and approximate the expectation value by

$$\langle Z \rangle \approx \frac{n_0 - n_1}{N_\mathrm{shots}}, \tag{17}$$

where n_k is the number of measurements returning $|k\rangle$, and N_shots is the number of measurements performed. For systems of N qubits, Eq. (17) generalizes to

$$\left\langle Z \otimes I^{\otimes(N-1)} \right\rangle \approx \frac{1}{N_\mathrm{shots}} \left(\sum_{k=0}^{2^{N-1}-1} n_k - \sum_{k=2^{N-1}-1}^{2^N-1} n_k \right), \tag{18}$$

where k is the decimal representation of the quantum state, i.e. for $N = 4$, $k = 8$ corresponds to $|1000\rangle$. The first sum runs over the measurements corresponding to states with eigenvalues $\lambda = +1$, while the second sum runs over the measurements corresponding to states with eigenvalues $\lambda = -1$. Due to the choice of $\mathcal{M} = Z \otimes I^{\otimes(N-1)}$ as our measurement basis, the

states with positive eigenvalue are exactly the first half of the possible outcomes, whereas the states with negative eigenvalue are the latter half of the possible outcomes. By the law of large numbers, Eq. (18) converges to the exact expectation value in the limit $N_{\text{shots}} \to \infty$, and the error in the approximation scales as $\mathcal{O}\left(1/\sqrt{N_{\text{shots}}}\right)$ [7]. While simulating the quantum circuits on a classical computer, we can achieve an arbitrarily small error by choosing N_{shots} to be sufficiently large, however, on a NISQ device, the results will always be affected by noise.

4. Minimization algorithms

As for all algorithms based on the variational principle, the VQE algorithm seeks to minimize the expecation value of the Hamiltonian with respect to the variational parameters $\boldsymbol{\theta}$. When opting for the hardware-efficient ansatz, the variational parameters enter the quantum circuit through rotational matrices $R_x(\theta_i)$ and $R_y(\phi_i)$. Classical minimization algorithms are often based on gradient descent methods, which need either an analytical or numerical evaluation of the gradient. In our case, the partial derivative of the expectation value with respect to parameter θ_i can be shown analytically to be

$$\frac{\partial \langle H \rangle}{\partial \theta_i} = \frac{\langle H(\theta_i + \pi/2) \rangle - H(\theta_i - \pi/2)}{2} \quad [11]. \qquad (19)$$

The simplest iterative approach for updating the variational parameters is the standard gradient descent, where the parameters are updated according to

$$\boldsymbol{\theta}^j = \boldsymbol{\theta}^{j-1} - \kappa \nabla_{\boldsymbol{\theta}^{j-1}} \langle H \rangle ,$$

where $\boldsymbol{\theta}^j$ is the value of the variational parameters at iteration j, $\nabla_{\boldsymbol{\theta}^j} \langle H \rangle$ is the vector with elements given by Eq. (19), and κ is the learning rate. One then updates the variational parameters iteratively until convergence in the parameters is reached. In practice, it is often convenient to approximate the gradient numerically [1].

IV. RESULTS

We use a self-written simulator and our implementation of the VQE to calculate the ground state energies of the previously introduced Hamiltonians. For the one-qubit systems, we also use one of IBM's publicly available quantum devices. Depending on availability, we use either `ibmq_belem`, `ibmq_lima`, `ibmq_quito`, or `ibmq_manila` which all have 5 qubits. Even with the analytic expression for the gradient given by Eq. (19), we opt for Powell's method which estimates the gradient using finite differences [10].

1. Simple many-body Hamiltonians

For the first two-dimensional many-body Hamiltonian given by Eq. (1), we use the VQE algorithm to calculate the ground state energy as a function of the interaction strength. We run our calculations with $N_{\text{shots}} = 2^{12} = 4096$, use the Powell minimization algorithm, and create our ansatz for the ground state by a combination of parameterized R_x and R_y gates. Using classical eigenvalue solvers, we compare our results with the analytic expression for the ground state energy. For the parameters in the Hamiltonian, we fix the non-interactive energies to $E_0 = 0.0$ and $E_1 = 4.0$, and $V_{11} = 3, V_{22} = -3$, and set $V_{12} = V_{21} = 0.2$ in the interactive part of the Hamiltonian. This corresponds to setting $\mathcal{E} = 2, \Omega = 2, c = 0, \omega_z = 3.0$, and $\omega_x = 0.2$. Fig. (5) shows the ground state energy for this system

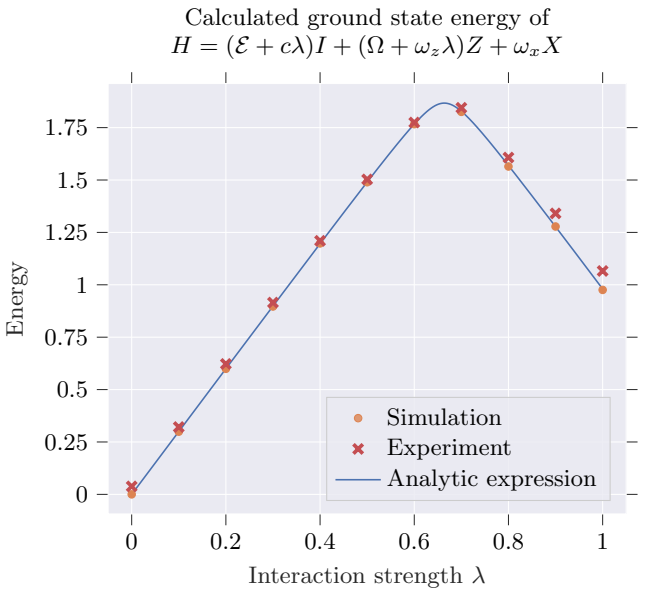

FIG. 5. Calculated ground state energy for the Hamiltonian given by Eq. (1) as a function of interaction strength λ. The solid line is the analytic expression and the points are values obtained by the VQE algorithm. The orange points are the results of a quantum device simulation, whereas the red points are calculated with one of IBM's publicly available NISQ devices. We use the values $\mathcal{E} = 2, \Omega = 2, c = 0, \omega_z = 3.0$, and $\omega_x = 0.2$ in the Hamiltonian.

as a function of the interaction strength. We note that the simulation is able to calculate the analytical eigenvalues exactly, but some deviations appear for the calculations on the quantum devices. This is most likely due to noise in the quantum device, and we have not done any error mitigation to minimize the deviations. Also, it appears that the errors in the experimental data increase with the interaction strength as the ground state is shifted more and more from $|0\rangle$ to an arbitrary linear combination of $|0\rangle$ and $|1\rangle$.

We repeat the calculation for the four-dimensional Hamiltonian given by Eq. (2). For the parameters in the Hamiltonian, we use non-interacting energies $\epsilon_{00}, \epsilon_{01}, \epsilon_{10}, \epsilon_{11} = 0.0, 2.5, 6.5, 7.0$ and interaction parameters $H_z = 3.0$ and $H_x = 2.0$. This corresponds to setting $\alpha = 4.0, \beta = -0.75, \gamma = -2.75$, and $\delta = -0.5$. We use the Powell minimization algorithm and calculate the expectation values with our simulation using $N_{\text{shots}} = 10^4$. Fig. (6) shows the simulated energies and the exact ground state energy as functions of the interaction strength. In both Fig. (5) and Fig. (6) we

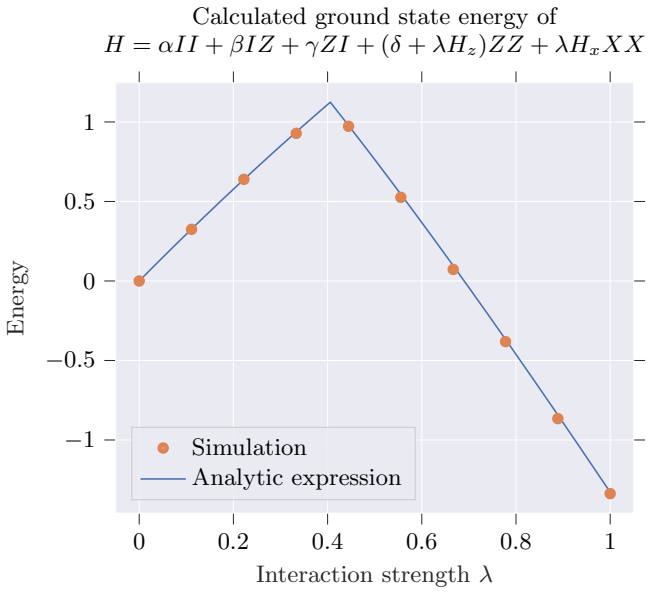

FIG. 6. Calculated ground state energy for the Hamiltonian given by Eq. (2) as a function of interaction strength λ. The solid line is the analytic expression and the points are values obtained by the VQE algorithm. For the calculations, we used the values $\alpha = 4.0, \beta = -0.75, \gamma = -2.75, \delta = -0.5, H_z = 3.0$, and $H_x = 2.0$ in the Hamiltonian.

see a level-crossing of the ground state energy as the interaction strength increases. We investigate this behavior further by calculating the von Neumann entropy of the ground state of the four-dimensional Hamiltonian as a function of the interaction strength. The von Neumann entropy of a state $|\psi\rangle$ can be calculated by

$$S(\rho) = -\sum_j \mu_j \log(\mu_j),$$

where $\rho = |\psi\rangle\langle\psi|$ is the density matrix of the state, μ_j are the non-zero eigenvalues of ρ, and the logarithm is base 2. The entropy of the ground state of the two-qubit Hamiltonian is shown in Fig. (7). The entropy increases with the interaction strength, showing that the mixing and the entanglement of the ground state increases when the many-body interaction is more present. Moreover, the entropy makes a larger jump around the value of λ which gives a level-crossing in the ground state energy.

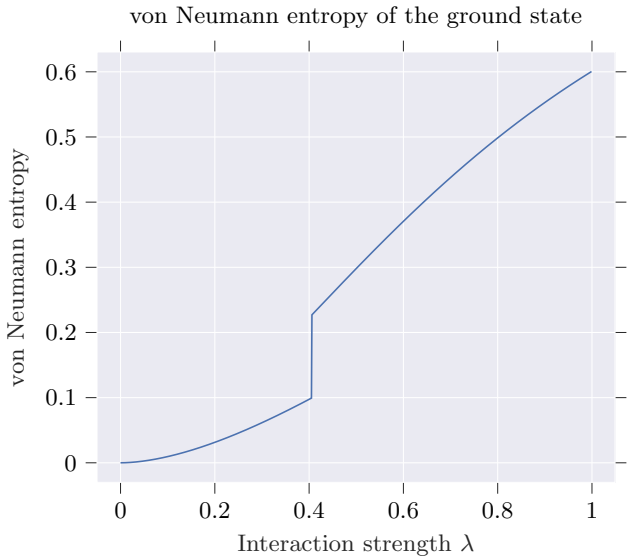

FIG. 7. von Neumann entropy for the ground state of the Hamiltonian given by Eq. (2) as a function of interaction strength λ.

This shows that many-body states have a large degree of mixing and entanglement and that the degree of entanglement is determined by the strength of the interaction matrix elements.

2. Lipkin model

For the Lipkin model, we scale the Hamiltonian by the single-particle energy ϵ, and calculate the ground state energy as a function of the dimensionless interaction strength V/ϵ. We compute the ground state energy with both the individual and the coupled spin mapping. For the individual spin mapping, we use the hardware-efficient ansatz and for the coupled spin mapping, we use the ansatz preparation which preserves the symmetries of the ground state given in Fig. (3). For both simulations, we use the Powell minimization algorithm and $N_{\text{shots}} = 10^4$ for the simulations. For the Lipkin model with total spin $J = 1$, the calculated ground state energy as a function of the interaction strength is shown in Fig. (8). For the simulations, we use both mapping schemes, however, we only use the coupled spin mapping when running the calculations on IBM's devices. The calculations with the individual spin mapping are marked I in the figure and the calculations with the coupled spin mapping are marked C. From the figure, we see that all three calculations return energies that are close to the analytic values.

For the Lipkin model with total spin $J = 2$, the ground state energy as a function of the interaction strength is shown in Fig. (9). The results from the individual spin mapping are labeled I, and the results

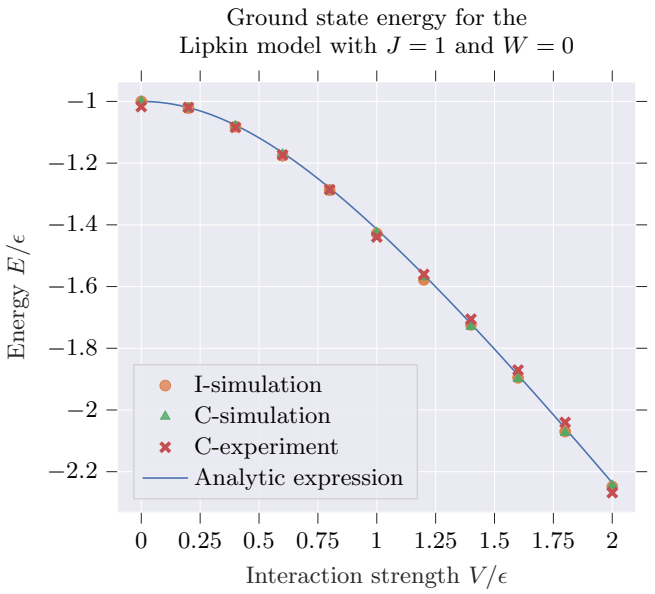

FIG. 8. Calculated ground state energy for the Lipkin model with total spin $J = 1$ without W-scattering as a function of interaction strength. The solid blue line is the analytic expression, and the points are calculated with the VQE algorithm. The orange points are the results of the calculations with the individual spin basis mapping and the green triangles are the results of the calculations with the coupled spin mapping. The red crosses are the results of calculations using IBM's quantum devices.

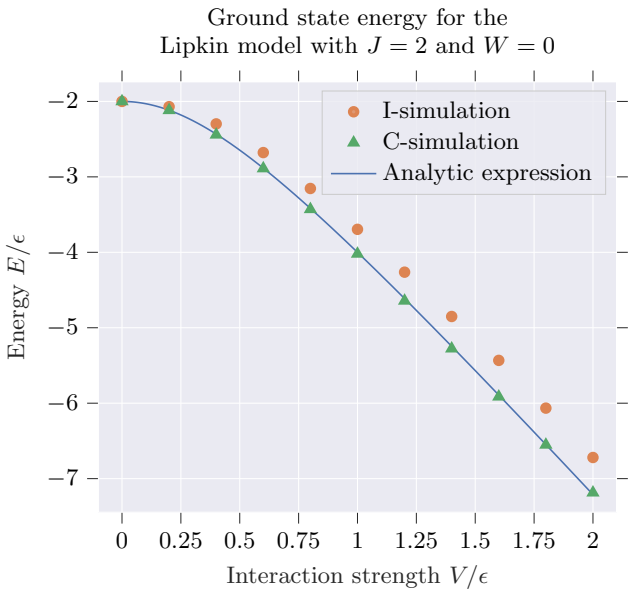

FIG. 9. Calculated ground state energy for the Lipkin model with total spin $J = 2$ without W-scattering as a function of interaction strength. The solid blue line is the analytic expression, and the points are calculated with the VQE algorithm. The orange points are the results of the calculations with the individual spin basis mapping and the green triangles are the results of the calculations with the coupled spin mapping.

obtained by the coupled spin mapping are labeled C. We note that the individual spin mapping is unable to find the correct ground state energy and that the deviations increase with the interaction strength. The analytic expression for the ground state energy, expressed in the individual spin mapping, is on the form

$$|\psi(\theta)\rangle = \cos^2\theta\,|0000\rangle + \sin^2\theta\,|1111\rangle - \frac{1}{\sqrt{12}}\sin 2\theta(|1100\rangle + |0011\rangle + |0101\rangle + |0110\rangle + |1001\rangle + |1010\rangle),$$

for some value of θ [5]. When we use the hardware-efficient state preparation, we are unable to isolate these eight states, and will therefore not reach the ground state. We sketch the proof of this statement in Appendix A. However, with the coupled spin basis, the state preparation given in Fig. (3) ensures that the ansatz has the correct symmetries spanning the subspace in which we find the ground state. We are therefore able to find the correct ground state energy via the coupled spin mapping, as shown in Fig. (9).

V. CONCLUSION

This work uses the VQE algorithm to study the ground state energy of interacting many-body Hamiltonians. Starting with two simple models for two- and four-dimensional systems with a tunable interaction strength, we see that both systems have a level-crossing at a particular value of the interaction strength. For the same systems, we calculate the von Neumann entropy and characterize the entanglement of the ground state. We observe that the entanglement increases with the interaction strength and makes a sudden jump at the level-crossing. We compute the ground state energy of the two-dimensional system using both a simulation and IBM's publicly available quantum devices. We experience some deviations between the simulated and experimental results, which we believe can be attributed to noise in the quantum device.

After studying the simple many-body models, we turn to the Lipkin model without W-scattering and total spin J. We use two different encoding schemes when rewriting the Lipkin model to a sum of Pauli strings. The individual spin mapping, which uses $N = 2J$ qubits to encode the system on a quantum device, is successful in finding the ground state energy for the $J = 1$ case, however, we do not obtain the correct ground state energy for $J = 2$. The failure of the individual spin mapping can be explained by the fact that the hardware-efficient

ansatz does not correctly represent the symmetries of the ground state. However, we find the correct ground state energy when using the coupled spin mapping, which uses $N = J$ qubits to encode the Lipkin model on a quantum device. For the case of $J = 1$, we use IBM's devices to run the experiments on quantum hardware and obtain close to the same results as in our simulations.

Further work could include experimental calculations with quantum devices on the Lipkin model of spin $J = 2$, possibly with error mitigation techniques. Besides, one could improve upon the work done in this article by including an error analysis of the results in order to quantify the deviations between the analytical and experimental values. It could also be of interest to study higher-dimensional Lipkin models using the same techniques we have covered in the present work. Additionally, one could include the W-scattering in the Lipkin model and study the dependence on both interaction parameters. Moreover, one could explore the possibilities of using different ansatz selections to find the correct ground state energy in the individual spin basis.

ACKNOWLEDGMENTS

We would like to thank IBM for making their quantum devices publicly available.

Appendix A: Inability to span the ground state of the Lipkin model with J = 2 and W = 0.

The ansatz constructed by the circuit in Fig. (4) does not span the ground state of the Lipkin model with total spin $J = 2$ and $W = 0$ when using the individual spin mapping. This appendix is dedicated to outlining the proof of this statement.

Every qubit starts out in state $|0\rangle$, and two rotational gates are applied to each qubit. After the rotations, qubit n is in the state

$$|\psi_n\rangle = A_n |0\rangle + B_n |0\rangle ,$$

where $A_n = \cos\theta_n/2 \cos\phi_n/2 + i \sin\theta_n/2 \sin\phi_n/2$ and $B_n = \cos\theta_n/2 \sin\phi_n/2 - i \sin\theta_n/2 \cos\phi_n/2$ are functions of the variational parameters. The entire system is in the state

$$\begin{aligned} |\Psi\rangle &= \bigotimes_{n=0}^{3} |\psi_n\rangle \\ &= A_0A_1A_2A_3 |0000\rangle + A_0A_1A_2B_3 |0001\rangle + \ldots + B_0B_1B_2B_3 |1111\rangle \end{aligned}$$

After the ladder of controlled-NOT gates, the state vector of the ansatz is

$$|\Psi_{\text{ansatz}}\rangle = A_0A_1A_2A_3 |0000\rangle + A_0A_1A_2B_3 |0001\rangle + \ldots + B_0B_1B_2B_3 |1010\rangle$$

The ground state of the Lipkin model with $J = 2$ without W-scattering is a superposition of states with an even number of particles with spin-up. In the individual spin mapping encoding scheme, this corresponds to bitstrings with an even Hamming weight and is on the form

$$|\psi_{\text{GS}}(\theta)\rangle = \cos^2\theta |0000\rangle + \sin^2\theta |1111\rangle - \frac{1}{\sqrt{12}} \sin 2\theta (|1100\rangle + |0011\rangle + |0101\rangle + |0110\rangle + |1001\rangle + |1010\rangle), \tag{A1}$$

for some value of θ [5]. Hence, we need the coefficients in front of the states in the ansatz with odd Hamming weights to be zero while having non-zero coefficients in front of the states with even Hamming weights. We see from Eq. (A1) that in the general case where neither $\cos\theta$ nor $\sin\theta$ equals 0, the ansatz must have non-zero coefficients in front of both $|0000\rangle$ and $|1010\rangle$. As the variational coefficient for $|0000\rangle$ is $A_0A_1A_2A_3$, and the the variational coefficient for $|1010\rangle$ is $B_0B_1B_2B_3$, this implies that none of the 8 variational coefficients can be zero. The ansatz will therefore always include states with both even as well as odd Hamming weights. Except for the non-interacting case with $V = 0$ and $|\psi_{\text{GS}}\rangle = |0000\rangle$, it is therefore not possible for the hardware-efficient ansatz constructed by the circuit in Fig. (4) to reach the ground state.

[1] Bartholomew-Biggs, M., Brown, S., Christianson, B., and Dixon, L. (2000). Automatic differentiation of algorithms. *Journal of Computational and Applied Mathematics*, 124(1):171–190. Numerical Analysis 2000. Vol. IV: Optimization and Nonlinear Equations.

[2] Berera, A. and Debbio, L. D. (2022). *Quantum Mechanics*. Cambridge University Press, Cambridge, United Kingdom.
[3] Bédos, E. (2022). *Notes on Elementary Linear Analysis*. Department of Mathematics, University of Oslo, Oslo.
[4] Feynman, R. P. (1982). Simulating physics with computers. *International Journal of Theoretical Physics*, 21:467–488.
[5] Hlatshwayo, M. Q., Zhang, Y., Wibowo, H., LaRose, R., Lacroix, D., and Litvinova, E. (2022). Simulating excited states of the lipkin model on a quantum computer. *Physical Review C*, 106(2).
[6] Hund, R. (2022). *Quantum Computing for Programmers*. Cambridge University Press, Cambridge, United Kingdom.
[7] Jensen, M. H. (2015). *Computational Physics: Lecture Notes Fall 2015*. Fysisk institutt UiO, Oslo.
[8] Lipkin, H., Meshkov, N., and Glick, A. (1965). Validity of many-body approximation methods for a solvable model: (i). exact solutions and perturbation theory. *Nuclear Physics*, 62(2):188–198.
[9] Peruzzo, A. (2014). A variational eigenvalue solver on a photonic quantum processor. *Nature Communications*, 5.
[10] Powell, M. J. D. (1964). An efficient method for finding the minimum of a function of several variables without calculating derivatives. *The Computer Journal*, 7(2):155–162.
[11] Schuld, M., Bergholm, V., Gogolin, C., Izaac, J., and Killoran, N. (2019). Evaluating analytic gradients on quantum hardware. *Phys. Rev. A*, 99:032331.
[12] Tilly, J., Chen, H., Cao, S., Picozzi, D., Setia, K., Li, Y., Grant, E., Wossnig, L., Rungger, I., Booth, G. H., and Tennyson, J. (2022). The variational quantum eigensolver: A review of methods and best practices. *Physics Reports*, 986:1–128. The Variational Quantum Eigensolver: a review of methods and best practices.